Electronic Supplementary Information

Hydrogen bond network structures of protonated short-chain alcohol clusters

Asuka Fujii,[*a] Natsuko Sugawara,[a] Po-Jen Hsu,[b] , Takuto Shimammori,[a]

Ying-Cheng Li,[b] Toru Hamashima,[a] and Jer-Lai Kuo[*b]

[a] Department of Chemistry, Graduate School of Science, Tohoku University, Sendai 980-8578, Japan.

[b] Institute of Atomic and Molecular Sciences, Academia Sinica, Taipei 10617, Taiwan.

* Corresponding authors: asukafujii@m.tohoku.ac.jp, jlkuo@pub.iams.sinica.edu.tw

Contents

Figure S1 Comparison between the observed IR spectrum of $H^+(MeOH)_5$-C_2H_2 and its simulations based on the linear and cyclic isomers. The simulations were performed at ωB97X-D/6-311++G(3df,3pd). Reprinted with permission from ref. 57 in the main text. Copyright 2016 American Chemical Society
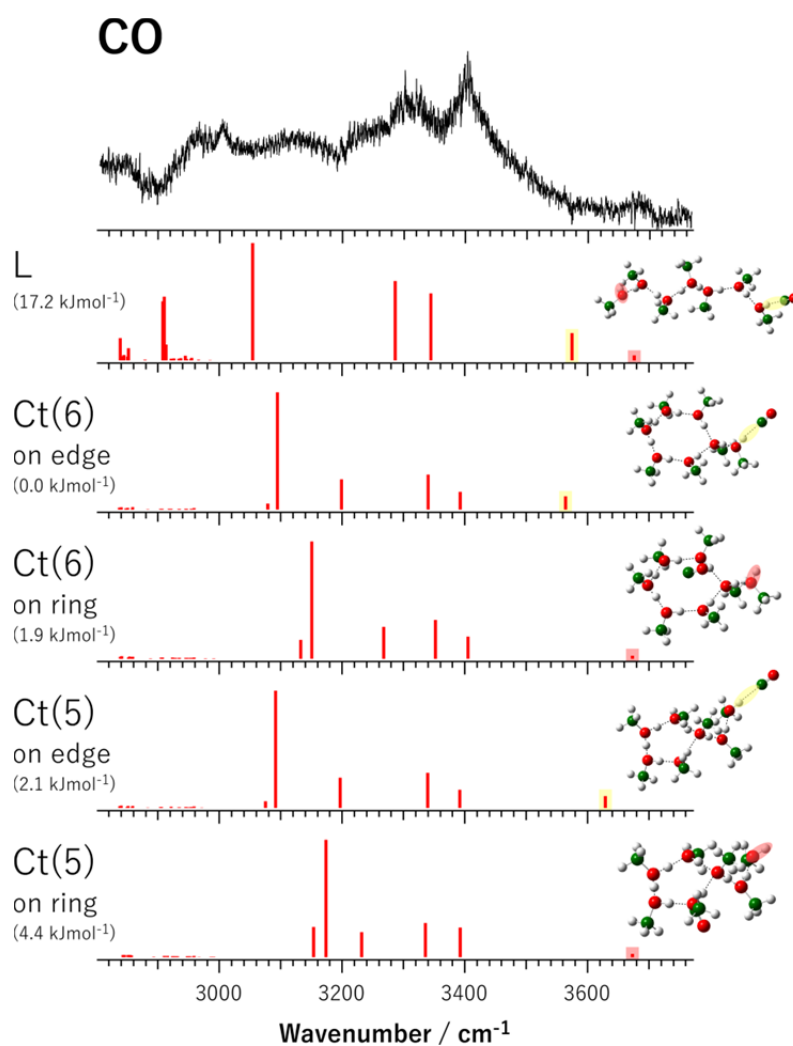
Figure S2   Comparison between the observed IR spectrum of $H^+(MeOH)_7$-CO and its simulations based on several low energy Ct and L type isomers.   Numbers in the parentheses are relative energy. Ct(n) means the H-bonded cyclic moiety forms an n-membered ring. The simulations were performed at $\omega B97X$-D/6-311++G(3df,3pd).
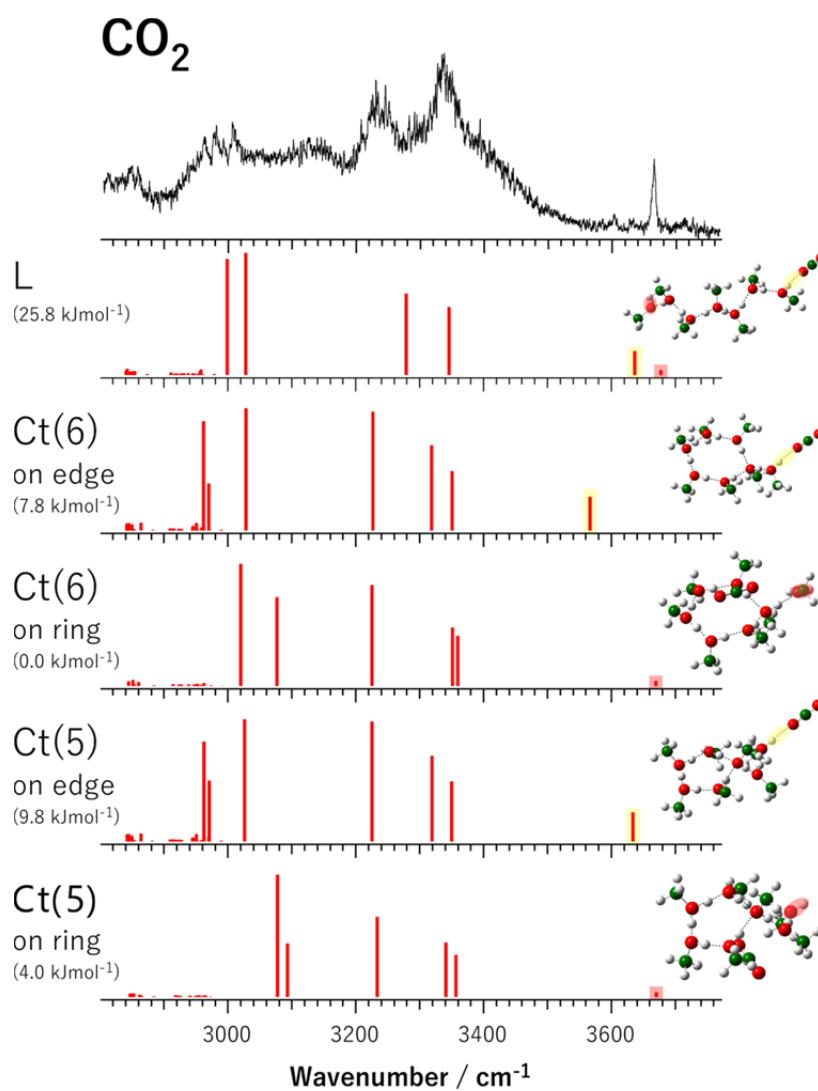
Figure S3   Comparison between the observed IR spectrum of $H^+(MeOH)_7$-CO_2 and its simulations based on several low energy Ct and L type isomers.   Numbers in the parentheses are relative energy.   The simulations were performed at ωB97X-D/6-311++G(3df,3pd).
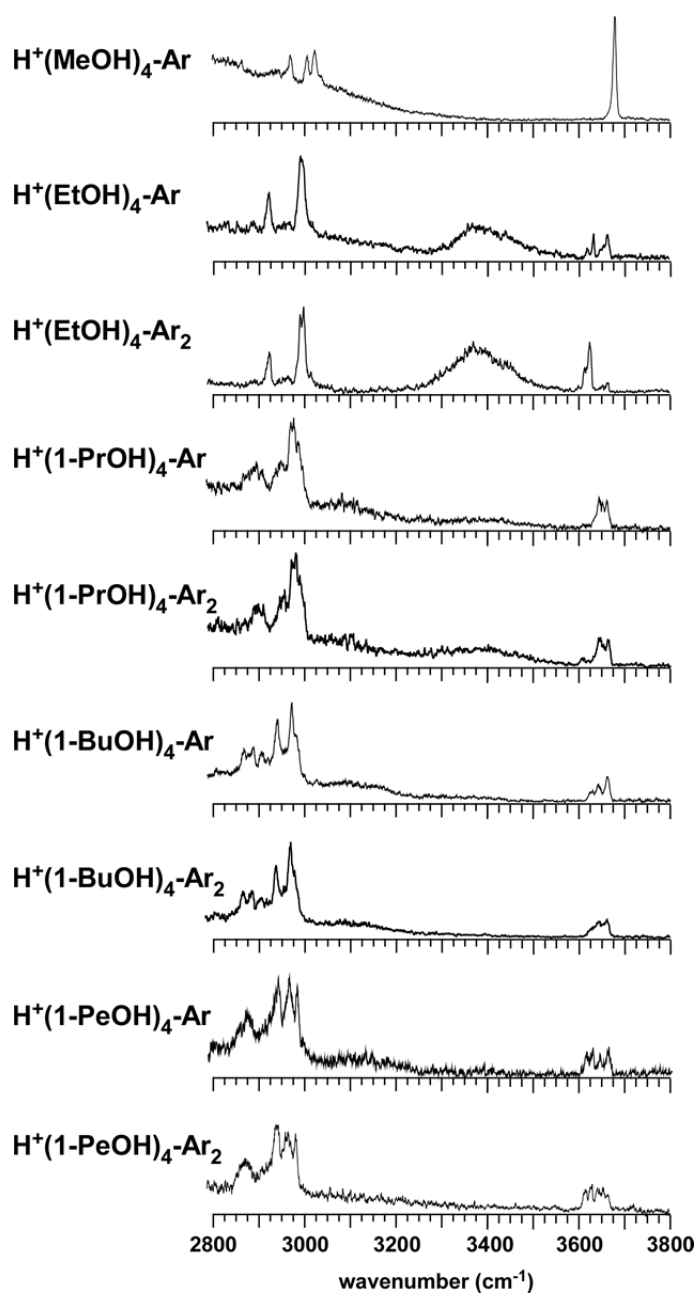
Figure S4 Observed spectra of $H^+(alcohol)_4$-Ar and $H^+(alcohol)_4$-Ar_2 in the OH and CH stretch region. EtOH, 1-PrOH, 1-BuOH, and 1-PeOH are ethanol, 1-propanol, 1-butanol, and 1-pentanol, respectively.
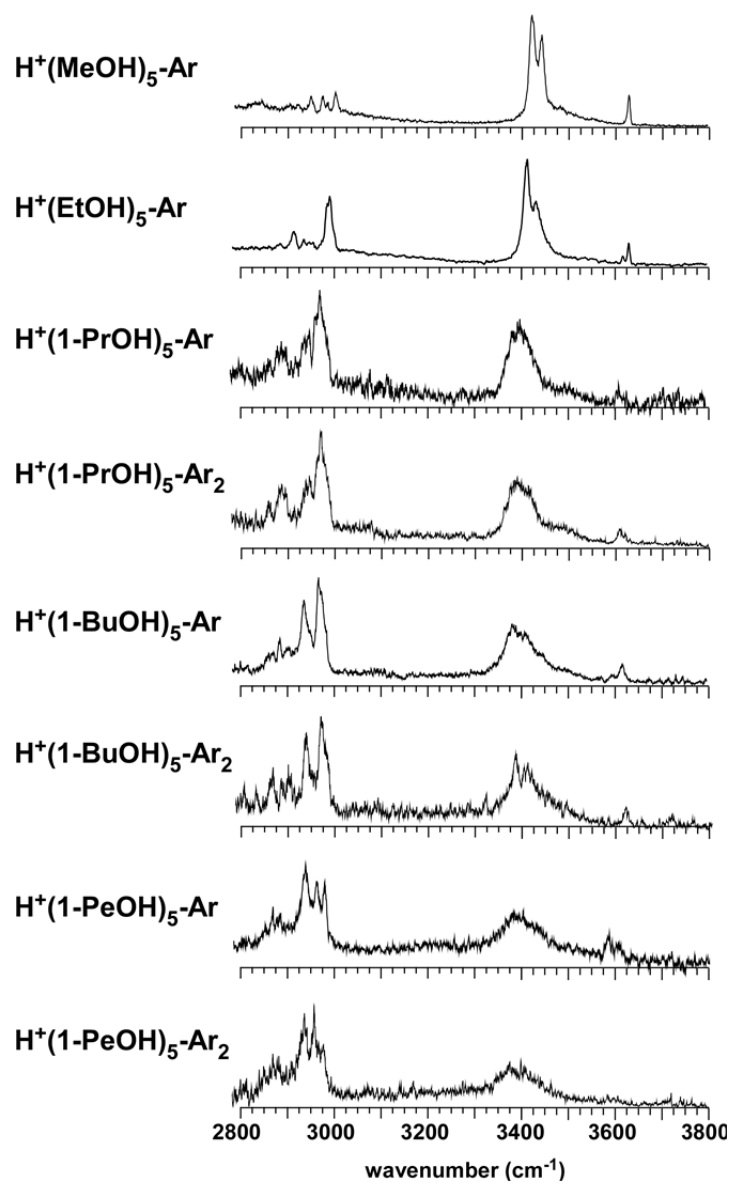
Figure S5   Observed spectra of $H^+(alcohol)_5$-Ar and $H^+(alcohol)_5$-Ar_2 in the OH and

CH stretch region.
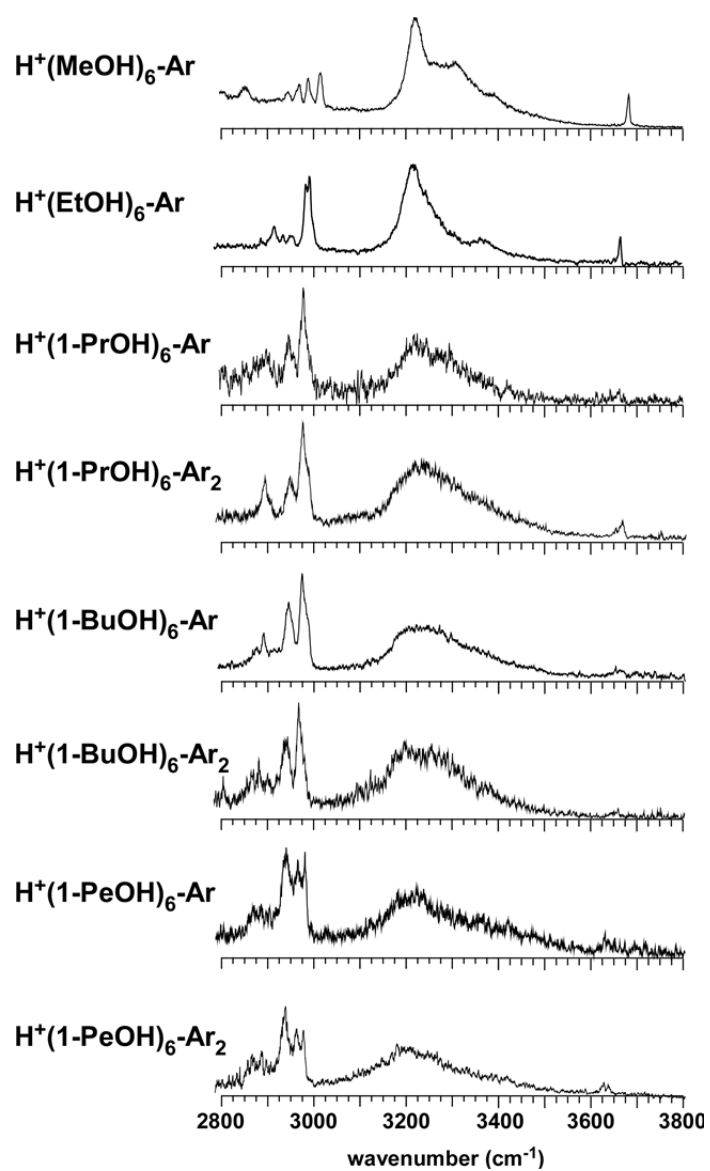
Figure S6 Observed spectra of $H^+(alcohol)_6$-Ar and $H^+(alcohol)_6$-Ar$_2$ in the OH and CH stretch region.
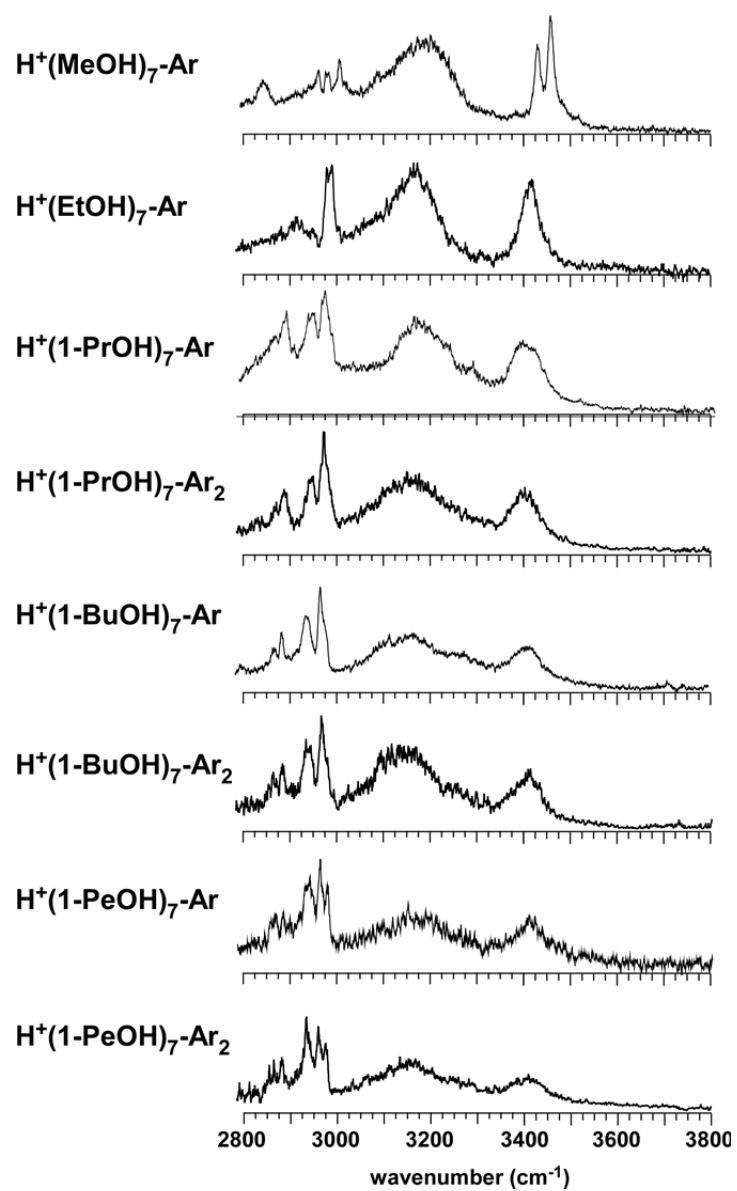
Figure S7 Observed spectra of H^+(alcohol)$_7$-Ar and H^+(alcohol)$_7$-Ar$_2$ in the OH and CH stretch region.

Details on the conformer search in $H^+(EtOH)_4$ and QHSA simulation of temperature dependence of the IR spectrum of $H^+(EtOH)_4$

Compare to methanol, the longer alkyl chain in ethanol possesses additional degrees of freedom. To access its influence, we have generated a database of 81 conformers from the structures protonated methanol tetramers with **L** and **C** types of hydrogen bond patterns.[1] An initial set of 81 structures can be constructed by replacing one of the hydrogen atoms on the CH_3 group of methanol. Furthermore, we have also generated additional 500 initial conformers with random orientations of the alkyl chain for unbiased configuration searching in both **L** and **C** types. In the former, we also rotate the torsion angle along the hydrogen bond. All in all, we have generated 1162 initial configurations for $H^+(EtOH)_4$ (581 for **L** and 581 for **C** forms). The random configurations may have unphysical distances between atoms.

These initial structures would go first through geometry optimization using three different DFT methods: (1) B3LYP/6-31+G*, (2) B3LYP/6-31+G* with D3 correction, and (3) ωB97X-D/6-311+G(2d,p). After geometry optimization, Hessians of the optimized structure were checked to ensure that they are local minima, and duplicates can be removed by checking their similarity index using a threshold of 0.99. [2, 3] As a result,

we obtained 508, 589, and 779 distinct isomers for the DFT methods 1, 2, and 3, respectively. Relative energies of two sets of structurally distinct **L** and **C** types are shown in the top panels of Fig. 13 in the main text. Even though we have the same number of initial structures, after screening out the duplicates, there are more structurally distinct **L** types than the **C** types. But these three DFT functionals cannot agree on which is the most stable conformers, **L** or **C**. In B3LYP/6-31+G*, **L** type isomers are more stable by ~ 0.6 kcal/mol. With range-separated functional, ωB97X-D/6-311+G(2d,p) also predicts the most stable conformer is an **L** type, but the relative energetics between the two groups is different in B3LYP/6-31+G* and ωB97X-D/6-311+G(2d,p). If empirical D3 dispersion is added to B3LYP/6-31+G*, B3LYP/6-31+G*-D3 predicts an opposite trend indicating that **C** forms are energetically more stable (also by ~ 0.6 kcal/mol).

To include the difference in the number of distinct isomers and vibrational free energy corrections, we evaluate thermal properties at elevated temperatures by engaging QHSA (quantum harmonic superposition approximation). In QHSA, contributions from vibrational modes to free energy are treated with harmonic approximation and all isomers are included according to their relative energetics. [4, 5] Temperature dependence of the population of the two types of hydrogen bond network is summarized in the lower panels in Fig. 13 in the main text. With B3LYP/6-31+G*, the **L** types dominate the whole

temperature range. Even with dispersion interaction included either by ωB97X-D/6-311+G(2d,p) or B3LYP/6-31+G*+D3 methods, **L** types also dominate in high-temperature range. These two DFT functionals, however, show very different temperature dependence. In the next paragraph, we will discuss simulated IR spectra based on these two DFT functionals.

In ωB97X-D/6-311+G(2d,p) and B3LYP/6-31+G*+D3, harmonic frequencies are rescaled by factors of 0.937 and 0.973, respectively. These scaling factors are determined to reproduce the free OH stretch bands of the clusters observed in experiments. For the homogeneous width, we broadened free OH with 20 cm^{-1}. Vibrational frequencies less than 3600 cm^{-1} belong to either H-bonded OH stretching or CH stretching mode. The latter is not the main issue here, so we adopted a power law formula (($\Gamma = \alpha(\omega_{freeOH} - \omega)^{\beta}$)) proposed by Takahashi and co-worker for all vibrational modes below 3600 cm^{-1}. [6, 7] To be consistent with our previous work, we used the same value with $\alpha = 0.0009$, $\beta = 1.9$ and $\omega_{freeOH} = 3678$ cm^{-1}.

The experimental spectra of neat and Ar-tagged H^{+}(EtOH)$_4$ are shown in the left panels of Fig. S8. In Ar-tagged clusters (colder conditions), there are two distinct peaks of free O-H stretching and a relatively broader band centered at ~3400 cm^{-1}. In neat clusters (warmer conditions), the free OH peaks shift to high frequency and the broad band at ~

3400 cm^{-1} is replaced by a diffused band centered at ~ 3000 cm^{-1}. The vibrational spectra

predicted by these two DFT functionals are shown in Fig. S8, while both methods show

different temperature dependence. Both methods agree that (1) the H-bonded OH band at

~3400 cm^{-1} is the marker band of the **C** types, (2) the diffused band ~ 3000 cm^{-1} can be

seen from the **L** types, and (3) free O-H stretching modes in the **L** types are higher in

frequency than their counterparts in the **C** types.

Based on our extensive structural search and preliminary testing on three DFT

functionals, the obtained experimental spectra with different internal energies suggest

that the structure change in protonated ethanol is a result of balance between the

hydrogen-bond strength and dispersion. The sensitive dependence on the conformation

with respect to thermal energy makes this cluster an ideal system to benchmark of the

accuracy of DFT calculations.

<u>References</u>
1. Y. –C. Li, T. Hamashima, R. Yamazaki, T. Kobayashi, Y. Suzuki, K. Mizuse, A. Fujii, J. –L. Kuo, *Phys. Chem. Chem. Phys*. 2015, **17**, 22042.
2. P. J. Ballester, P. W. Finn, and W. G. Richards, *J. Mol. Graphics Modell.*, 2009, **27**, 836.
3. E. –P. Lu, P. –R. Pan, Y. –C. Li, M. –K. Tsai, J. –L. Kuo, *Phys. Chem. Chem. Phys.* 2014, **16**, 18888.
4. D. Bing, T. Hamashima, A. Fujii, J. –L. Kuo, *J. Phys. Chem. A*, 2010, **114**, 8170.
5. M. Katada, P. –J. Hsu, A. Fujii, J. –L. Kuo, *J. Phys. Chem. A* 2017, **121**, 5399.
6. Y. L. Cheng, H. Y. Chen, K. Takahashi, *J. Phys. Chem. A* 2011, **115**, 5641.
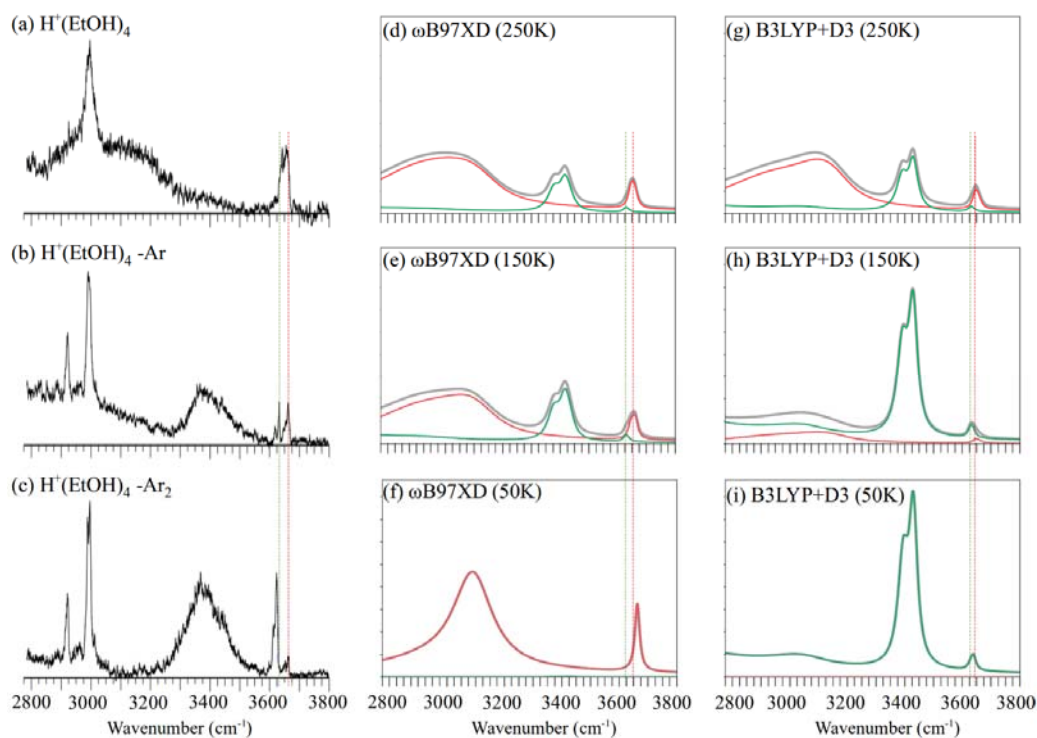7. M. Morita, K. Takahashi, *Phys. Chem. Chem. Phys.* 2012, **14**, 2797.

Figure S8 Left panels: experimental IR spectra of $H^+(EtOH)_4$: (a) neat $H^+(EtOH)_4$, (b) $H^+(EtOH)_4$-Ar, and (c) $H^+(EtOH)_4$-Ar$_2$. Center panels: IR spectra of $H^+(EtOH)_4$ simulated with QHSA based on local minima optimized by ωB97X-D/6-311+G(2d,p) at different temperatures (d) 250K, (e) 150K, and (f) 50K. Right panels: IR spectra of $H^+(EtOH)_4$ simulated with QHSA based on local minima optimized by B3LYP/6-31+G*+D3 at different temperatures (g) 250K, (h) 150K, and (i) 50K.